Mol Neurobiol (2012) 46:361–373
DOI 10.1007/s12035-012-8294-5

Genotypic Association of the *DAOA* Gene with Resting-State Brain Activity in Major Depression

Jun Chen · Yong Xu · Juan Zhang · Zhifen Liu · Cheng Xu · Kerang Zhang · Yan Shen · Qi Xu

Received: 19 April 2012 / Accepted: 21 June 2012 / Published online: 1 August 2012

Abstract Compelling evidence suggests that the glutamatergic system may contribute to the pathophysiology of major depression (MDD). While the D-amino acid oxidase activator (*DAOA*) gene can affect glutamatergic function, its genetic associations with MDD and abnormal resting-state brain activity have yet to be elucidated. A total of 488 patients with MDD and 480 controls were recruited to examine MDD association for the *DAOA* gene in a Chinese population, of whom 53 medication-free patients and 46 well-matched controls underwent resting-state functional magnetic resonance imaging for regional homogeneity (ReHo) analysis. The differences in ReHo between genotypes of interest were initially tested by the Student's *t* test, and the 2×2 (genotypes×disease status) ANOVA was then performed to identify the main effects of genotypes, disease status, and their interactions in MDD. Allelic association of the *DAOA* gene with MDD was observed for rs2391191, rs3918341, and rs778294 and haplotypic association for 2- and 3-SNP haplotypes. Six clusters in the cerebellum, right middle frontal gyrus and left middle temporal gyrus showed genotypic association between altered ReHo and rs2391191. The main effects of rs2391191 genotypes were found in the right culmen and right middle frontal gyrus. The left uvula and left middle temporal gyrus showed a genotypes×disease status interaction. Our results suggest that the *DAOA* gene may confer genetic risk of MDD. Genotypic effect of rs2391191 and its interaction with disease status may contribute to the altered ReHo in patients with MDD. Glutamatergic modulation may play an important role in alteration of the resting-state brain activities.

Keywords Major depression · D-amino acid oxidase activator · Resting-state functional magnetic resonance imaging · Regional homogeneity · Genotypic association

Jun Chen and Yong Xu contributed equally to this study.
This work was performed at the National Laboratory of Medical Molecular Biology, Institute of Basic Medical Sciences, Chinese Academy of Medical Sciences and Peking Union Medical College

Electronic supplementary material The online version of this article (doi:10.1007/s12035-012-8294-5) contains supplementary material, which is available to authorized users.

J. Chen · J. Zhang · Y. Shen · Q. Xu (✉)
National Laboratory of Medical Molecular Biology, Institute of Basic Medical Sciences, Chinese Academy of Medical Sciences, and Peking Union Medical College, Tsinghua University,
No.5 Dong Dan San Tiao,
Beijing 100005, People's Republic of China
e-mail: xuqi@pumc.edu.cn

Y. Xu · Z. Liu · K. Zhang (✉)
Department of Psychiatry, First Hospital of Shanxi Medical University,
Taiyuan 030002, People's Republic of China
e-mail: krzhang_sxmu@vip.163.com

C. Xu
Department of MRI, Shanxi Provincial People's Hospital,
Taiyuan 030002, People's Republic of China

Introduction

Major depression (MDD) is a severe psychiatric disease and is predicted to become the second leading cause of disability by 2020 [1]. Previous studies to examine the neurobiological mechanism underlying MDD have focused on the monoaminergic system [2]. However, increasing evidence indicated that neurochemical abnormalities in MDD might not be attributable only to monoaminergic system dysfunction [3, 4]. Meanwhile,

several lines of evidence have demonstrated strong association of the glutamatergic system with MDD, suggesting a role of the glutamatergic system in the pathophysiology of MDD [5–7].

The D-amino acid oxidase activator (*DAOA*) gene, which was initially identified as a susceptibility locus for schizophrenia [8], is thought to interact with the gene coding for D-amino acid oxidase (*DAO*) that is involved in the metabolism of D-serine by acting as a coactivator of the glycine binding site on the glutamatergic *N*-methyl D-aspartate (NMDA) receptor [9] and subsequently influences NMDA excitatory transmission [10]. These findings suggest that the *DAOA* gene may lead to abnormal glutamatergic levels by affecting function of the NMDA receptors via modulating D-serine metabolism [11, 12]. An epistatic relationship between *DAO* and *DAOA* has also been reported [13]. Recent studies implicated that the *DAOA* gene might be involved in the dendritic arborization [14].

A number of studies have tried to identify homogenous subgroups of a disease in order to define quantitative intermediate phenotypes (also termed endophenotype) [15]. Imaging genetics has been developed to examine association of genetic variation with neuroimaging endophenotypes, in which resting-state functional magnetic resonance imaging (rs-fMRI) is an approach frequently applied to investigate mental disorders [16]. Several methods can be used to analyze the rs-fMRI data, such as regional homogeneity (ReHo), functional connectivity and amplitude of low frequency fluctuation although they are quite different from each other [17–19].

The Kendall's coefficient of concordance (KCC) has been used as an index of ReHo, which assumes that brain activity is likely to present in clusters rather than a single voxel and the neighboring voxels are temporally similar [20]. By measuring regional coherence of a given voxel with its nearest neighbors, ReHo can indicate some unexpected hemodynamic responses that model-driven methods (such as general linear model) may fail to discover by rs-fMRI [17]. Unlike other data-driven method (such as ICA and PCA), ReHo needs no assumptions of the spatial independence [21] while it can be used to reduce the number of voxels and to select the ideal "seed" [22]. Extensions of this method to group analysis are conceptually and practically straightforward [23]. Accordingly, ReHo may fully stand for the nature of the resting-state data and can be used to investigate resting-state activities in the human brains. ReHo has been increasingly employed to investigate various psychiatric disorders [24, 25], suggesting that it is potentially useful in revealing the pathophysiology of psychiatric disorders during resting state.

The present study was designed on the basis of the hypothesis that the *DAOA* gene may be genetically associated with abnormal resting-state brain activity in patients with MDD. This was a two-stage study that initially focused on testing associations of the *DAOA* gene with MDD in 488 patients and 480 control subjects, and then examined the functional roles of a disease-associated variant in neuroimaging changes in patients with MDD.

Materials and Methods

Subjects

A total of 488 unrelated sporadic patients with MDD (209 males and 279 females), aged 37.6±10.3 years, and 480 control subjects (214 males and 266 females), aged 36.8±11.0 years, were recruited for genetic analysis. All the patients were recruited as inpatients by First Hospital of Shanxi Medical University and clinically diagnosed as having MDD by at least two experienced psychiatrists according to the DSM-IV criteria [26]. The control subjects were recruited from local communities. Written informed consent to attend this study was obtained from all subjects (for patients it came from their first-degree relatives) prior to inclusion in the study, as approved by the Ethics Committee of Chinese Academy of Medical Sciences and Peking Union Medical College.

Fifty-three first-episode medication-free patients and 46 control subjects, who were included in genetics analysis, underwent rs-fMRI scanning. Inclusion criteria were as follows: aged 18–50 years, right handed, total 17-item Hamilton Depression Rating Scale (HDRS) score of no less than 15 for patients, and ability to give voluntary informed consent, no cardiovascular and metallic implants. Individuals with the following conditions were excluded: psychiatric disorders other than depression, history of neurological illness (e.g., epilepsy), brain trauma with loss of consciousness, alcoholism, drug and other substance abuse in the past 6 months, currently taking any prescription or centrally acting medications, pregnant or breastfeeding, other major medical illness, and other contraindications to fMRI scanning. Demographic information and disease severity for the subjects are given in Table S1 in the Electronic Supplementary Material (ESM).

Genotyping of SNPs

Ten single nucleotide polymorphisms (SNPs) present in a 95-Kb region of the *DAOA* gene were selected from the NCBI SNP database (www.ncbi.nlm.nih.gov/SNP) and the HapMap database (www.hapmap.org), including

rs3916965 (M12), rs3916966 (M13), rs3916967 (M14), rs2391191 (M15), rs3918341 (M16), rs9558562, rs947267 (M18), rs778294 (M19), rs3918342 (M23), and rs1421292 (M24). Of these ten SNPs, M12, M13, M14, M23 and M24 are intergenic; M15 and rs9558562 are non-synonymous (M15 leads to a Lys30Arg change and rs9558562 leads to a Glu62Lys change); and M16, M18, and M19 are intronic (M19 becomes exonic in isoform 2). All the SNPs selected have a minor allele frequency (MAF) of 5 % (except for rs9558562) based on the NCBI SNP database.

Genomic DNA was extracted from peripheral blood leukocytes using a standard phenol/chloroform method. Individual genotypes of the tested SNPs were determined by bi-directional sequencing (ABI 3700DNA sequencer; PerkinElmer, Applied Biosystems, Foster City, CA, USA) following PCR amplification. Chromas software (Technelysium Pty., Ltd., Version 2.22, Tewantin, Australia) was used for the genotype calling (the genotype call rate was 96.6 % on average); 10 % duplicates of randomly chosen samples were used for quality control, and none showed replicate error. The conditions used for genotyping these SNPs are given in Tables S2 and S3 in the ESM.

Analysis of Genotyping Data

Linkage disequilibrium (LD) between paired SNPs was estimated by the Haploview software (version 4.1; Broad Institute of MIT and Harvard, Cambridge, MA, USA) and expressed as D' and r^2 [27]. The Hardy–Weinberg equilibrium (HWE) was tested based on the genotypic distributions of individual SNPs by using the goodness-of-fit χ^2 test. Allelic and haplotypic associations with MDD were analyzed using the UNPHASED software (version 3.1; Dudbridge F, MRC Biostatistics Unit, Cambridge, UK). In our study, the sliding window size for haplotype analysis were 2 and 3, and 10,000 permutations were performed to obtain a global P value corrected for all alleles and haplotypes tested. Power analysis with the log additive mode was performed using the QUANTO software (http://hydra.usc.edu/gxe), in which the prevalence of MDD was set at 16.2 %, the false positive rate at α=0.05, and the frequency of minor allele at 0.113 (except rs9558562) in the control groups.

MRI Data Acquisition

A SIEMENS TRIO 3-T scanner was used to collect the fMRI data. Subjects were instructed to lie down on the bench while putting their head in a birdcage head coil, took a few minutes to adjust themselves to the dark environment before scanning, then keep still and relaxing with their eyes closed, not to concentrate on anything in particular. Soft pads and earplugs were used when scanning to restrict head motion and reduce scanner noise. Scanning stopped immediately if the subjects did not feel comfortable and could not continue scanning. The scanning sequences were as follows: (1) T1-weighted axial image: with repetition time/echo time (TR/TE)=580/18 ms, thickness/gap=4/0 mm, matrix=256×144, and field of view (FOV)=192×192 mm; (2) T1-weighted whole brain images: with a 3D-FLASH sequence, TR/TE=14/4.92 ms, thickness/gap=1.5/0.3 mm, matrix=256×192, FOV=230×230 mm, flip angle=25°, 120 slices; and (3) rs-fMRI scan: with echo planar imaging pulse sequence, TR/TE=2000/30 ms, thickness/gap=4/0 mm, matrix=64×64, FOV=192×192 mm, flip angle=90°, 33 slices, 248 time points which lasted about 8 min.

Image Data Pre-processing and ReHo Analysis

All the image data were reconstructed and inspected by two experienced radiologists for quality controls. Image preprocessing and individual ReHo analysis with the KCC method as previously described [17], were performed using the DPARSF software (version 2.0; Yan Chao-Gan, State Key Laboratory of Cognitive Neuroscience and Learning, Beijing Normal University, Beijing, China). The first 10 volumes were discarded and the remaining were slice timing and head motion corrected (anyone who had more than 1.0 mm of translation and 1.0° of rotation would be excluded), spatially normalized to Montreal Neurological Institute space according to the standard EPI template, then linearly detrended and band-pass filtered (0.01–0.08 HZ); finally, a KCC map was calculated in a voxel-by-voxel way that was then divided by the mean KCC of the whole brain and smoothed by a 4*4*4 FWHM Gaussian kernel to obtain a ReHo map. Accordingly, data corrections for six head movement parameters, global mean signal, white matter and cerebrospinal fluid signals were performed.

To analyze a difference in ReHo between genotypes of interest, the Student's t test was applied to identify a genotype that might be involved in alteration of ReHo in either patients with MDD or the control subjects. To avoid excessive correction, statistical threshold for this analysis was set at $P<0.001$ and clusters size of >20. After this analysis, whole clusters around the significant peak voxel coordinate were respectively saved as region of interest (ROI) for future analysis.

Inference on Main Effects and Interactions of Genotypes and Disease Status

A general linear model 2×2 (genotypes×disease status) ANOVA was performed in the SPM8 (Welcome Department

of Cognitive Neurology, London, UK) to investigate the main effects of genotypes of interest, disease status, and their interactions within ROIs. Post hoc analysis was then conducted to investigate the signal source of these effects in paired subgroups. Because the *t* test has reduced sensitivity in small search regions, false discovery rate (FDR) correction was used within these ROIs. Finally, the ReHo values within ROIs were extracted by using the REST software (introduced by Song et al., http://www.restfmri.net) for each subject, allowing these measures to be used for Figures in the Prism software (GraphPad Software.inc).

Results

Association Analysis

Genotypic distributions of these ten SNPs were all in HWE, and three LD blocks spanning between M12 and rs9558562, between M18 and M19, and between M23 and M24 were observed, which was similar to those in previous studies.

Power calculation showed that our sample had 84.28 % power to detect allelic association of OR=1.5 at a false rate of 0.05 (except rs9558562 for its MAF<5 %).

An association signal was detected at rs2391191 (M15, unadjusted P=0.01), rs3918341 (M16, unadjusted P=0.04), and rs778294 (M19, unadjusted P=0.02), but such associations did not survive the correction with 10,000 permutations (adjusted P=0.08). All haplotypes used for analysis had a frequency of >1 % in either patients or the control subjects. The 2-SNP haplotype analysis showed strong associations for M12-M13 (χ^2=37.63; df=3; unadjusted P<0.001), M13-M14 (χ^2=12.36; df=3; unadjusted P=0.006), and M18-M19 (χ^2=19.17; df=3; unadjusted P<0.001). The 3-SNP haplotype analysis also showed disease association for M12-M13-M14 (χ^2=37.63; df=3; unadjusted P<0.001), M13-M14-M15 (χ^2=14.63; df=3; unadjusted P=0.002), and M14-M15-M16 (χ^2=16.68; df=6; unadjusted P=0.01). Results are given in Fig. 1 and Tables 1, 2, and 3.

Differences in ReHo between rs2391191 Genotypes

Because rs2391191 produced the strongest association signal in the above association analysis and its non-synonymous base change leads to Lys30Arg substitution, this SNP was considered as a putative functional variant to test the differences in ReHo between its genotypes [28]. To increase power, four genetic subgroups were defined as AA carriers (23 patients and 23 controls) and G+ carriers (AG+GG; 30 patients and 23 controls) as only five GG carriers were found in the patient group and three GG carriers in the control group. Comparison of the differences in ReHo between the AA and G+ carriers in MDD identified four clusters with significantly decreased ReHo in the left uvula (T=−4.27; df=51), the right pyramis (T=−4.14; df=51) and the bilateral culmen (T=−4.04; df=51 and T=−4.13; df=51, respectively) in the G+ carriers, while two clusters with significantly increased ReHo were found in the right middle frontal gyrus (T=3.94; df=51) and the left middle temporal gyrus (T=4.56; df=51). No significant result was observed in controls at this SPM threshold. Results are given in Fig. 2 and Table 4.

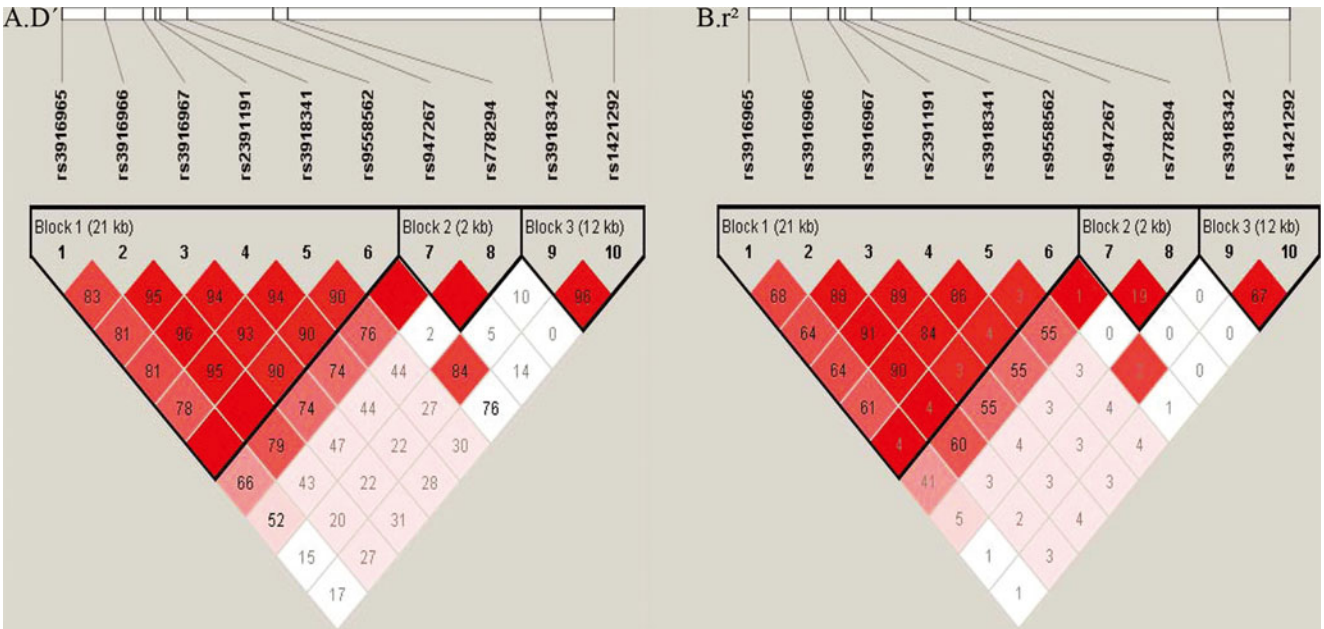

Fig. 1 LD structures of the ten SNPs genotyped in the *DAOA* gene. The LD strengths between paired SNPs are shown in *color*

Table 1 Allelic associations of the SNPs tested in the *DAOA* gene with MDD

SNP	MDD (%)			CON (%)			MAF (%)		Allelic	OR
	M/M	M/m	m/m	M/M	M/m	m/m	MDD	CON	P^a (df=1)	
M12	29.81	52.85	17.34	35.32	47.48	17.20	43.76	40.94	0.22	1.12
M13	30.31	51.55	18.14	36.05	46.94	17.01	43.92	40.48	0.14	1.15
M14	29.83	52.79	17.38	35.50	48.95	15.55	43.78	40.02	0.09	1.16
M15	29.10	51.84	19.06	36.99	47.66	15.35	44.98	39.18	0.01	1.27
M16	31.63	50.53	17.83	34.78	48.48	18.74	43.10	40.98	0.04	1.09
X	91.06	8.51	0.44	93.83	6.17	0.00	4.68	3.09	0.07	1.54
M18	34.87	51.26	13.87	36.36	49.05	14.59	39.50	39.11	0.86	1.02
M19	71.93	26.40	1.67	78.48	20.46	1.06	14.86	11.29	0.02	1.37
M23	30.70	45.63	23.67	26.98	50.32	22.70	46.48	47.86	0.55	0.94
M24	37.27	48.86	13.87	35.52	49.26	15.22	38.30	39.85	0.49	0.94

SNP single nucleotide polymorphism, *CON* the control group, *MDD* the patient group, *OR* odds ratio, *MAF* minor allele frequency, *X* rs9558562, *M* the major allele, *m* the minor allele

[a]Uncorrected *P* value, while adjusted *P* value from 10,000 permutations was 0.08

Effects of rs2391191Genotypes, Disease Status, and their Interactions

The 2×2 (genotypes×disease status) ANOVA within six ROIs showed a significant main effect of rs2391191 genotypes in the right culmen ($F_{1,\ 95}$=12.14; P^{FDR}=0.02) and the right middle frontal gyrus ($F_{1,\ 95}$=17.67; P^{FDR}=0.02). Post hoc analysis revealed that this main effect resulted from decreased ReHo in the right culmen (T=−4.08; df=51; P^{FDR}=0.002) and increased ReHo in the right middle frontal gyrus (T=3.95; df=51; P^{FDR}=0.002) in the G+ carriers compared with the AA carriers in MDD. However, at this SPM threshold (P<0.05; FDR corrected and cluster size, >10); there was no main effect of rs2391191 genotypes in other four regions and no main effect of disease status within six ROIs in a comparison between controls and patients.

The 2×2 ANOVA also revealed significant interactions between rs2391191genotypes and disease status in the left uvula ($F_{1,\ 95}$=9.46; P^{FDR}=0.01) and the left middle temporal gyrus ($F_{1,\ 95}$=13.31; P^{FDR}=0.03). Post hoc analysis suggested that a disease status effect might occur in the left middle temporal gyrus based on the ReHo differences between the AA carriers of controls and patients (T=4.46; df=44; P^{FDR}=0.03). Meanwhile, decreased ReHo in the left uvula (T=−4.34; df=51; P^{FDR}=0.001) and increased ReHo in the left middle temporal gyrus (T=4.58; df=51; P^{FDR}=0.002) were also observed in the G+ carriers compared with the AA carriers in MDD. In addition, the control G+ carriers showed higher ReHo in the left middle temporal gyrus than

Table 2 Association of 2-SNP haplotypes with MDD

Combination	Haplotype[a]	MDD N	CON N	OR	Individual P values	Global P value (df=3)
M12-M13	1-1	487.90	446.60	1.00	0.95	<0.001
	1-2	11.09	32.40	0.16	<0.001	
	2-1	7.09 35.4	35.40	0.08	<0.001	
	2-2	375.90	297.60	0.95	0.01	
M13-M14	1-1	487.00	510.80	1.00	0.38	0.006
	1-2	5.02	10.18	0.52	0.20	
	2-1	3.02	15.18	0.21	0.005	
	2-2	371.00	339.80	1.15	0.09	
M18-M19	1-1	550.70	569.00	1.00	0.42	<0.001
	1-2	17.27	0.00	7.40e+008	<0.001	
	2-1	249.30	260.00	0.99	0.12	
	2-2	122.70	105.00	1.21	0.37	
M19-M23	1-1	411.80	431.70	1.00	0.54	0.04
	1-2	377.20	388.30	0.83	0.33	
	2-1	84.22	48.26	1.16	0.005	
	2-2	52.78	55.74	0.63	0.57	

CON the control group, *MDD* the patient group, *OR* odds ratio

[a]"1" represents the major allele and "2" represents the minor allele

Table 3 Association of 3-SNP haplotypes with MDD

Combination	Haplotype[a]	MDD *N*	CON *N*	OR	Individual *P* values	Global *P* values
M12-M13-M14	1-1-1	469.90	437.30	1.00	0.86	<0.001 (*df*=3)
	1-1-2	2.99	5.36	0.52	1.00	
	1-2-1	2.02	4.83	0.39	1.00	
	1-2-2	8.07	27.50	0.27	<0.001	
	2-1-1	5.07	32.58	0.14	<0.001	
	2-1-2	2.02	2.75	0.68	1.00	
	2-2-1	0.99	6.28	0.15	1.00	
	2-2-2	352.90	289.40	1.14	0.03	
M13-M14-M15	1-1-1	466.60	503.80	1.00	0.03	0.002 (*df*=3)
	1-1-2	20.42	4.02	5.48	0.001	
	1-2-1	4.00	6.03	0.72	1.00	
	1-2-2	1.02	4.18	0.26	1.00	
	2-1-1	2.09	8.02	0.28	1.00	
	2-1-2	0.93	7.19	0.14	1.00	
	2-2-1	13.36	13.18	1.09	0.96	
	2-2-2	357.60	325.60	1.19	0.17	
M14-M15-M16	1-1-1	489.50	514.60	1.00	0.20	0.01 (*df*=6)
	1-1-2	3.98	12.09	0.35	0.04	
	1-2-1	17.41	3.88	4.72	0.004	
	1-2-2	5.14	10.42	0.52	0.19	
	2-1-1	4.05	5.97	0.71	1.00	
	2-1-2	15.50	16.33	1.00	0.83	
	2-2-1	9.07	8.54	1.12	0.82	
	2-2-2	361.40	332.20	1.14	0.18	

CON the control group, *MDD* the patient group, *OR* odds ratio

[a]"1"represents the major allele and "2" represents the minor allele

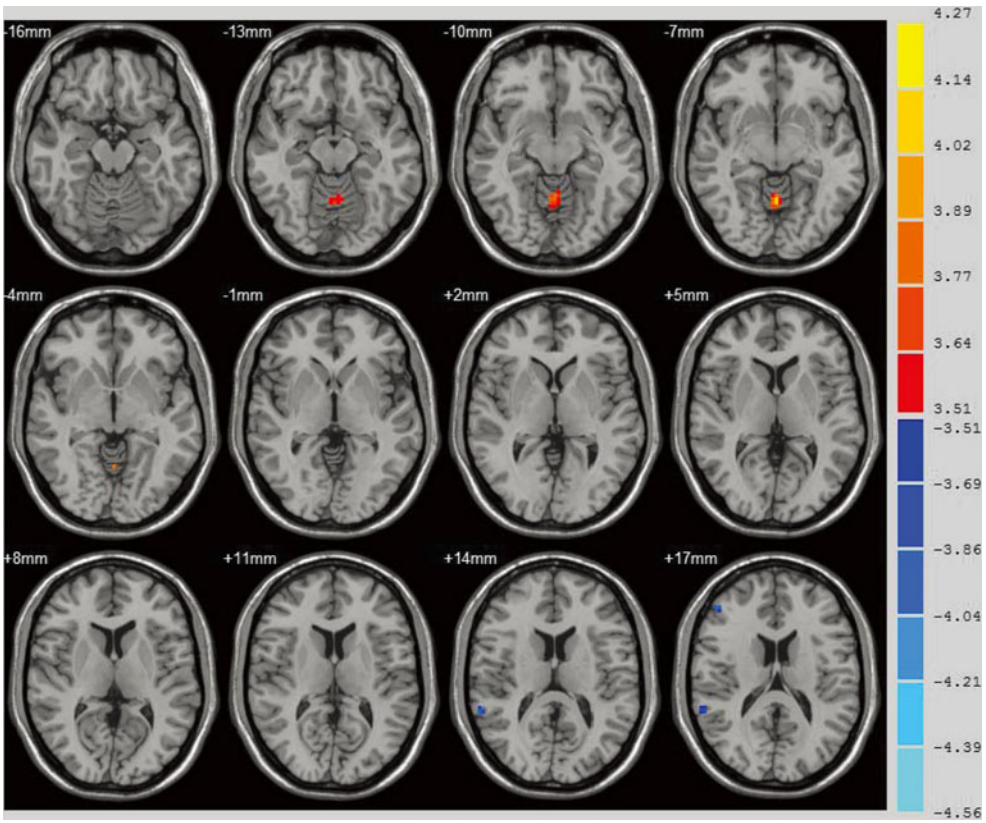

Fig. 2 Differences in ReHo between rs2391191 genotypes in the cerebellum, right middle frontal gyrus, and left middle temporal gyrus in patients with MDD. *Color bar* represents the peak *T* values

Table 4 Six clusters revealing genotypic association between ReHo alteration and rs2391191 in patients with MDD

Brain area	L/R	BA	Talairach coordinate			Number of voxels	Peak *T* value[a]
			x	*y*	*z*		
Uvula	L	–	−9	−65	−27	31	−4.27
Pyramis	R	–	12	−68	−27	43	−4.14
Culmen	R	–	15	−42	−18	22	−4.04
Culmen	L	–	0	−55	−2	72	−4.13
middle frontal gyrus	R	BA46	48	42	17	21	3.94
middle temporal gyrus	L	BA21	−50	5	−20	20	4.56

Voxel coordinates represent the peak voxel in local maxima. $P<0.001$; cluster size, >20

L left, *R* right, *BA* Brodmann area

[a]Comparison between G+ and AA carriers in MDD

(T=3.28; df=44; P^{FDR}=0.03) the AA carriers with MDD. Results are given in Tables 5 and 6, and Figs. 3, 4, 5, and 6.

Discussion

The *DAOA* Association with MDD

The *DAOA* gene was first reported to be associated with schizophrenia in Canadian and Russian samples by Chumakov and co-workers [8]. However, a genetic overlap may exist across the major psychiatric diseases such as bipolar disorder, MDD and schizophrenia [29, 30]. It has been previously reported that a haplotype containing rs2391191 was associated with depression [31]; a possible association of the *DAOA* gene with major mood episodes was also reported [32]. Our study showed a similar result by detection of association signals at three SNPs, four 2-SNP haplotypes and three 3-SNP haplotypes but indicated that the G allele of rs2391191 might contribute to the risk of MDD, which is consistent with the results from studies conducted by Chumakov in schizophrenia. However, inconsistency could not be neglected [33]. There may be many reasons for the inconsistency, including the type I errors, different genetic backgrounds (due to different ethnicities), study designs (e.g., sample size, sampling bias, and family based vs. population based), polygenic inheritance, as well as phenotypic and genomic heterogeneity [34]. The strong LD as shown in Fig. 1 raises the possibility that the regions from M12 to M15 and from M18 to M19 may contain variants generating the association signal, and their combined effects should also be taken into account.

The *DAOA* Association with Altered ReHo in MDD

Recent studies found that rs2391191 was associated with impaired verbal memory and reduced cortical thickness in schizophrenia [28, 35]. Furthermore, this SNP was also found to be associated with low visuospatial ability in bipolar disorder [36]. Our analysis showed genotypic association of rs2391191 with altered ReHo by identifying the differences in ReHo between the rs2391191 genotypes in six clusters in patients with MDD; subsequent analysis within these ROIs confirmed that this alternation resulted from the main effect of genotype and its interaction with disease status.

It has been thought that the glutamate cycling consumes 60–80 % of overall brain energy [37]. A brain default mode network (DMN; a group of specific brain

Table 5 Four clusters revealing main effect of genotypes or interaction effect within ROIs

Brain area	L/R	BA	Talairach coordinates			Number of voxels	Peak *F* value
			x	*y*	*z*		
Uvula	L	–	−9	−68	−24	27	9.46[a]
Culmen	R	–	15	−42	−18	19	12.14[b]
Middle frontal gyrus	R	BA46	50	42	15	16	17.67[b]
Middle temporal gyrus	L	BA21	−50	5	−20	11	13.31[a]

Voxel coordinates represent the peak voxel in local maxima. $P<0.05$, false discovery rate corrected; cluster size, >10

L left, *R* right, *BA* Brodmann area

[a] Interaction effect between genotypes and disease status

[b] Main effect of genotypes

Table 6 Clusters exhibiting differences in ReHo between subgroups classified by rs2391191 genotypes

Brain area	L/R	BA	Talairach coordinates			Number of voxels	Peak *T* value
			x	*y*	*z*		
Uvula	L	–	−6	−68	−27	26	−4.34[a]
Culmen	R	–	15	−39	−21	19	−4.08[a]
Middle frontal gyrus	R	BA46	48	42	17	15	3.95[a]
Middle temporal gyrus	L	BA21	−50	5	−20	11	4.58[a]
Middle temporal gyrus	L	BA21	−50	−4	−25	11	4.46[b]
Middle temporal gyrus	L	BA21	−51	0	−27	10	3.28[c]

Voxel coordinates represent the peak voxel in local maxima. $P<0.05$, false discovery rate corrected; cluster size, >10

L left, *R* right, *BA* Brodmann area

[a] Comparison between G+ and AA carriers in MDD

[b] Comparison between AA carriers in controls and AA carriers with MDD

[c] Comparison between G+ carriers in controls and AA carriers with MDD

areas activated mainly in the resting state, cognitively demanding and externally cued tasks can attenuate its activity in the resting state), including the middle frontal/temporal gyrus [38], may be controlled by the glutamatergic system [39, 40]. A possible link between the *DAOA* gene, abnormal glutamate level and cognitive performance has been observed in both patients with MDD and rat models [41–43]. Accordingly, we hypothesize that combination of specific genotype(s) of the *DAOA* gene and other unknown factors may lead to abnormal glutamatergic levels that may be involved in the aberrant brain energy metabolism, cognitive deficit and abnormal DMN, leading to the altered ReHo in MDD.

MDD-Related Alteration of ReHo in the Cerebellum and Middle Frontal Gyrus

Recent studies have demonstrated that glutamate and NMDA receptor activation may cause cerebellar dysfunction and the cerebellum may play a potential role in cognition [44, 45]. A significantly decreased ReHo has been found in this area in patients with MDD compared with their first-degree relatives [46]. Our study confirmed that the right culmen and left uvula had decreased ReHo in the G+ carriers compared with the AA carriers in MDD. The *DAOA* gene can be expressed in granular cells of the cerebellum and is related to mitochondrial fragmentation [14, 47], suggesting that abnormal expression of *DAOA* and

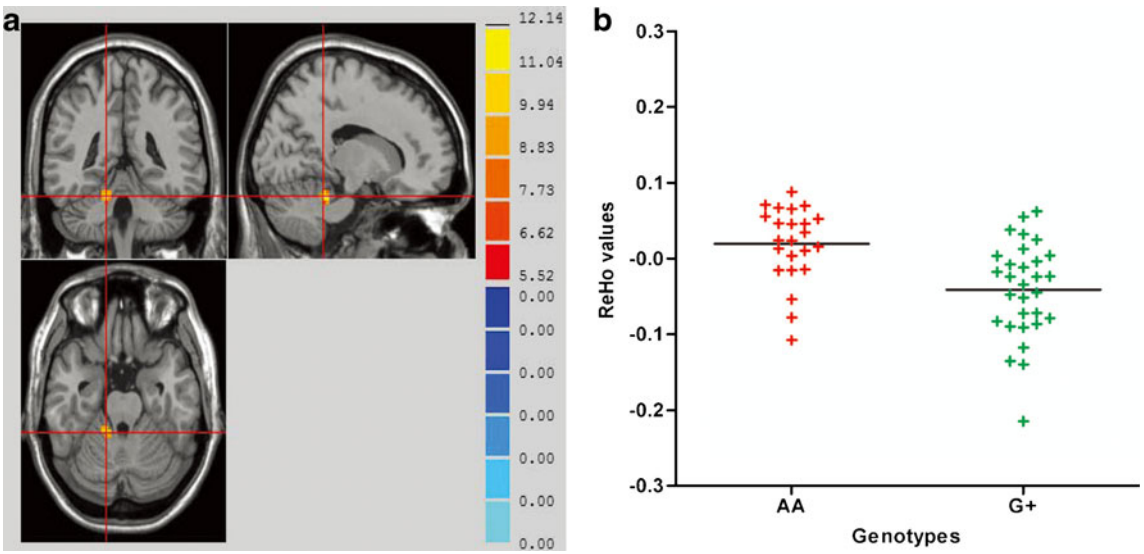

Fig. 3 Main effect of rs2391191 G+ genotype in the right clumen. **a** Clusters of significance for the main effect of G+ genotype in the right clumen ($P<0.05$, FDR corrected, and ten voxels minimum). *Color bar* represents the peak *F* values; **b** scatter plot for the comparison of G+ and AA carriers in patients with MDD. The *y*-axis displays the ReHo values within this ROI. *Lines* represent the mean ReHo values

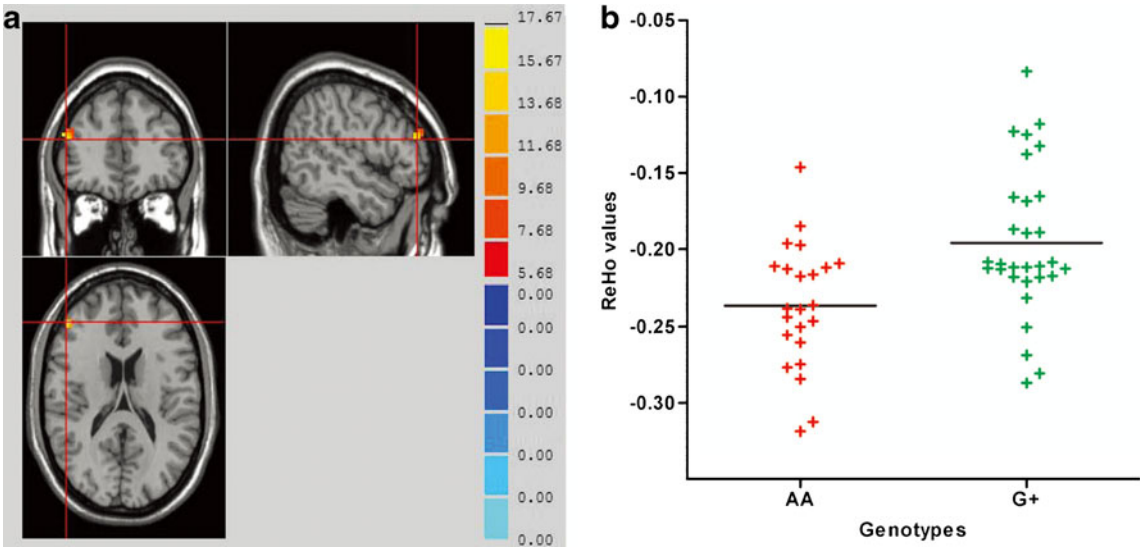

Fig. 4 Main effect of rs2391191 G+ genotype in the right middle frontal gyrus. **a** Clusters of significance for the main effect of G+ genotype in the right middle frontal gyrus ($P<0.05$, FDR corrected, and ten voxels minimum). *Color bar* represents the peak *F* values; **b** scatter plot for the comparison of G+ and AA carriers in patients with MDD. The *y*-axis displays the ReHo values within this ROI. *Lines* represent the mean ReHo values

altered energy-production may be the reason for a change of ReHo in MDD. Nevertheless, there was no significant difference in ReHo observed between the G+ carriers and the AA carriers in the control group, a compensatory mechanism such as protective role of the A allele may be involved. Meanwhile, no significant difference in ReHo was observed between the G+ carriers with MDD and those in controls, which may be due to small sample size of the GG carriers in both groups, and may in some extent confirm the risk of MDD resulted from the G allele.

A parametric Go/No-go task analysis revealed that patients with MDD had increased activations in the middle frontal gyrus in rejection trials [48]; the middle frontal gyrus that is responsible for verbal working memory critically could mediate character recognition in Chinese individuals [49]. The present study showed

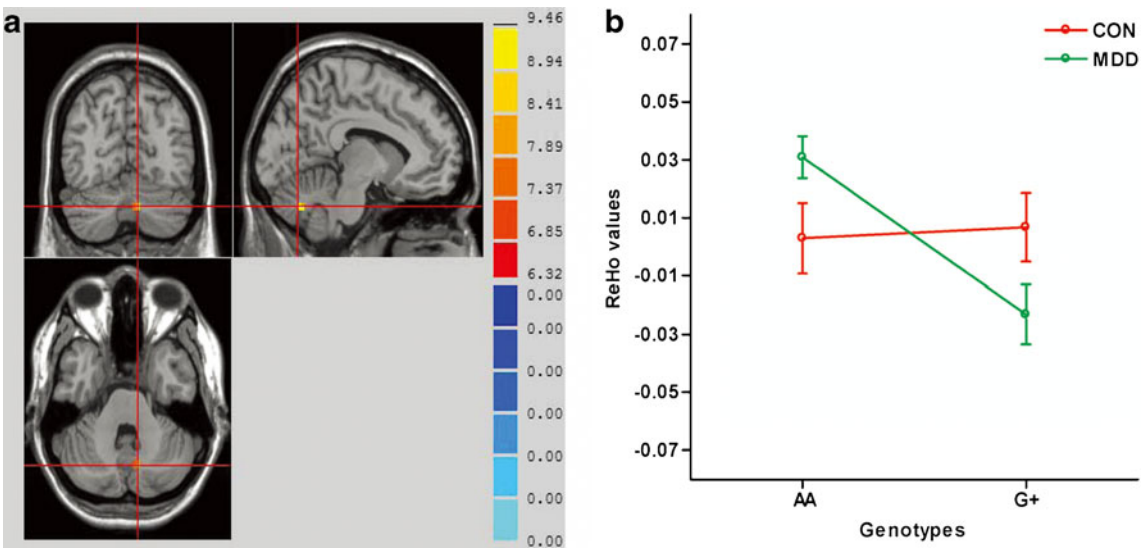

Fig. 5 The interaction between rs2391191 genotypes and disease status in the left uvula. **a** Clusters of significance for the interaction effect in the left uvula ($P<0.05$, FDR corrected, and ten voxels minimum). *Color bar* represents the peak *F* values; **b** interaction graph showing a ReHo difference between the genotypes, in which the G+ carriers have lower ReHo than the AA carriers with MDD. No significant disease status effect was observed at the same threshold. *Error bars* represent the standard error against the means. The *y*-axis displays the ReHo values within this ROI

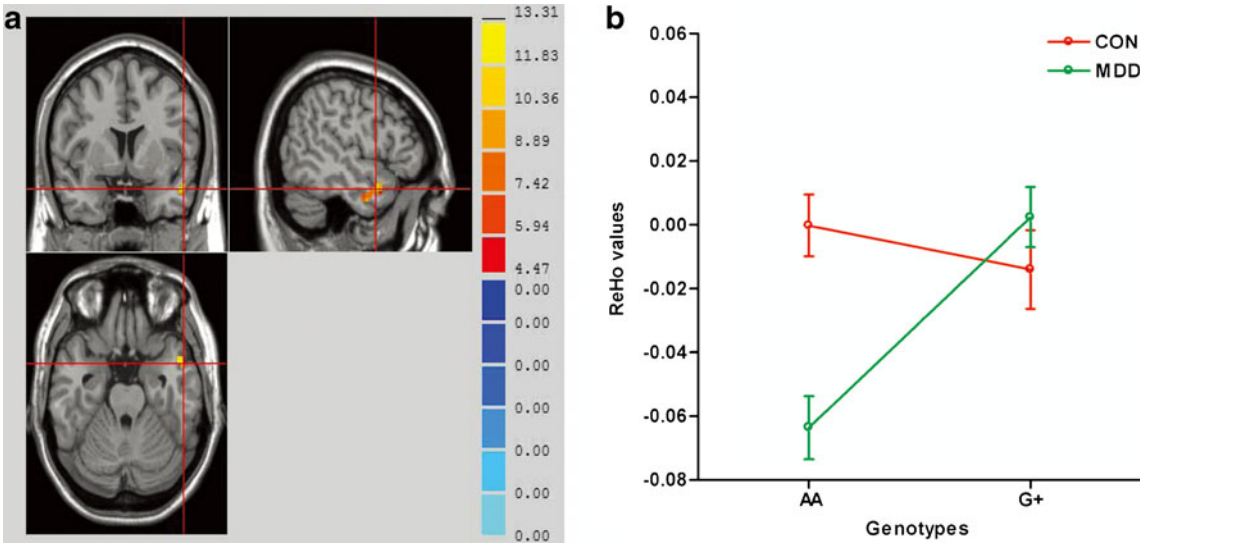

Fig. 6 The interaction between rs2391191 genotypes and disease status in the left middle temporal gyrus. **a** Clusters of significance for the interaction effect in the left middle temporal gyrus ($P<0.05$, FDR corrected, and ten voxels minimum). *Color bar* represents the peak *F* values; **b** interaction graph showing ReHo differences, in which the AA carriers have lower ReHo than the G+ carriers with MDD and controls of either the AA carriers or the G+ carriers. *Error bars* represent the standard error against the means. The *y*-axis displays the ReHo values within this ROI

increased ReHo in the middle frontal gyrus in the G+ carriers compared with the AA carriers in MDD, suggesting a positive main effect of the G+ genotype, although the G+ genotype is responsible for decreased ReHo in the cerebellum in MDD. This may be attributable to different roles and expression levels of the *DAOA* gene in disparate brain regions, different structural or functional bases (activities) of brain regions, and combined effects of the G+ genotype and other unknown factors.

Genotypes x Disease Status Interaction in the Middle Temporal Gyrus

The correlation between the polymorphisms of the *DAOA* gene and brain activation in the right middle temporal gyrus has been reported in a verbal fluency task in healthy individuals [50]. A recent rs-fMRI study described decreased ReHo in the left middle temporal gyrus in MDD patients [51]. The present study showed that the left middle temporal gyrus had a significant interaction between the disease status (decreased ReHo in the AA carriers with MDD compared with those in the controls) and the genotypes (increased ReHo in the G+ carriers compared with the AA carriers in MDD). However, it remains unknown how and when this interaction could alter ReHo in the middle temporal gyrus although many factors such as corticosteroids could influence the status of MDD [52]. Furthermore, expression of multiple genes involved in axonal growth/synaptic function was reduced in the middle temporal cortex in patients with MDD [53], and their interaction with the *DAOA* genotypes could make an alteration of ReHo in the middle temporal gyrus of MDD patients.

Altered Resting-State Brain Activity and Glutamatergic Modulation

Recent studies of MDD have demonstrated altered glutamate levels in resting state and a correlation between glutamate concentrations and resting-state hyperactivity in some regions (e.g., pgACC) [7, 54, 55]. Dysfunction of glutamatergic receptors has also been observed in antidepressant-treated animals [56, 57]. There is convergence for our assumption of the link between abnormal glutamatergic metabolism and alteration of brain resting-state activities in MDD. However, Northoff and co-workers found that resting-state activity may be indirectly regulated by glutamate [58]. Anyhow, glutamatergic modulation may play an important role in the alteration of resting-state brain activities.

There are a couple of potential limitations of our study. First, the sample size for imaging analysis is rather small so that the type II errors cannot be overcome. Second, the relationship between the brain regions tested and cognitive levels of patients was not investigated. A further study of combination of the *DAOA* gene and neuroimaging information is required to confirm our initial findings reported in this study.

Acknowledgments We sincerely thank all the subjects for their participation in this study. We also thank the Department of Psychiatry, First Hospital of Shanxi Medical University, Taiyuan, China and

Department of MRI, Shanxi Provincial People's Hospital, Taiyuan, China, for their help with recruitments of subjects and sample collection.

Financial Disclosure The work was supported by the research grants from the National Basic Research Program of China (2010CB529603and 2012CB517902), the National Natural Science Foundation of China (30971001, 30971054, 31021091, and 81171290), the Beijing Natural Science Foundation (7102109) and the Fok Ying Tong Education Foundation (121024). The sponsors had no role in the design and conduct of the study; collection, management, analysis, and interpretation of the data; or preparation, review, or approval of the manuscript. All the authors listed have read through the manuscript, approved for publication, and declared no conflict of interest. Jun Chen and Yong Xu had full access to all of the data in the study and took their responsibility for the integrity of the data and the accuracy of data analysis.

References

1. Murray CJ, Lopez AD (1996) Evidence-based health policy—lessons from the Global Burden of Disease Study. Science 274 (5288):740–743
2. Sumegi A (2008) Domino principle—monoamines in bottom-view. Neuropsychopharmacol Hung 10(3):131–140
3. Berton O, Nestler EJ (2006) New approaches to antidepressant drug discovery: beyond monoamines. Nat Rev Neurosci 7(2):137–151. doi:10.1038/nrn1846
4. Sen S, Sanacora G (2008) Major depression: emerging therapeutics. Mt Sinai J Med 75(3):204–225. doi:10.1002/msj.20043
5. Auer DP, Putz B, Kraft E, Lipinski B, Schill J, Holsboer F (2000) Reduced glutamate in the anterior cingulate cortex in depression: an in vivo proton magnetic resonance spectroscopy study. Biol Psychiatry 47(4):305–313. doi:S0006-3223(99)00159-6
6. Li CX, Wang Y, Gao H, Pan WJ, Xiang Y, Huang M, Lei H (2008) Cerebral metabolic changes in a depression-like rat model of chronic forced swimming studied by ex vivo high resolution 1H magnetic resonance spectroscopy. Neurochem Res 33(11):2342–2349. doi:10.1007/s11064-008-9739-0
7. Berman RM, Cappiello A, Anand A, Oren DA, Heninger GR, Charney DS, Krystal JH (2000) Antidepressant effects of ketamine in depressed patients. Biol Psychiatry 47(4):351–354. doi:S0006-3223(99)00230-9
8. Chumakov I, Blumenfeld M, Guerassimenko O, Cavarec L, Palicio M, Abderrahim H, Bougueleret L, Barry C, Tanaka H, La Rosa P, Puech A, Tahri N, Cohen-Akenine A, Delabrosse S, Lissarrague S, Picard FP, Maurice K, Essioux L, Millasseau P, Grel P, Debailleul V, Simon AM, Caterina D, Dufaure I, Malekzadeh K, Belova M, Luan JJ, Bouillot M, Sambucy JL, Primas G, Saumier M, Boubkiri N, Martin-Saumier S, Nasroune M, Peixoto H, Delaye A, Pinchot V, Bastucci M, Guillou S, Chevillon M, Sainz-Fuertes R, Meguenni S, Aurich-Costa J, Cherif D, Gimalac A, Van Duijn C, Gauvreau D, Ouellette G, Fortier I, Raelson J, Sherbatich T, Riazanskaia N, Rogaev E, Raeymaekers P, Aerssens J, Konings F, Luyten W, Macciardi F, Sham PC, Straub RE, Weinberger DR, Cohen N, Cohen D (2002) Genetic and physiological data implicating the new human gene G72 and the gene for D-amino acid oxidase in schizophrenia. Proc Natl Acad Sci U S A 99(21):13675–13680. doi:10.1073/pnas.182412499
9. Mustafa AK, Kim PM, Snyder SH (2004) D-serine as a putative glial neurotransmitter. Neuron Glia Biol 1(3):275–281. doi:10.1017/S1740925X05000141
10. Panatier A, Gentles SJ, Bourque CW, Oliet SH (2006) Activity-dependent synaptic plasticity in the supraoptic nucleus of the rat hypothalamus. J Physiol 573(Pt 3):711–721. doi:10.1113/jphysiol.2006.109447
11. Sacchi S, Bernasconi M, Martineau M, Mothet JP, Ruzzene M, Pilone MS, Pollegioni L, Molla G (2008) pLG72 modulates intracellular D-serine levels through its interaction with D-amino acid oxidase: effect on schizophrenia susceptibility. J Biol Chem 283 (32):22244–22256. doi:10.1074/jbc.M709153200
12. Schell MJ, Molliver ME, Snyder SH (1995) D-serine, an endogenous synaptic modulator: localization to astrocytes and glutamate-stimulated release. Proc Natl Acad Sci U S A 92(9):3948–3952
13. Corvin A, McGhee KA, Murphy K, Donohoe G, Nangle JM, Schwaiger S, Kenny N, Clarke S, Meagher D, Quinn J, Scully P, Baldwin P, Browne D, Walsh C, Waddington JL, Morris DW, Gill M (2007) Evidence for association and epistasis at the DAOA/G30 and D-amino acid oxidase loci in an Irish schizophrenia sample. Am J Med Genet B Neuropsychiatr Genet 144B(7):949–953. doi:10.1002/ajmg.b.30452
14. Kvajo M, Dhilla A, Swor DE, Karayiorgou M, Gogos JA (2008) Evidence implicating the candidate schizophrenia/bipolar disorder susceptibility gene G72 in mitochondrial function. Mol Psychiatry 13(7):685–696. doi:10.1038/sj.mp. 4002052
15. Bearden CE, Freimer NB (2006) Endophenotypes for psychiatric disorders: ready for primetime? Trends Genet 22(6):306–313. doi:10.1016/j.tig.2006.04.004
16. Raichle ME, MacLeod AM, Snyder AZ, Powers WJ, Gusnard DA, Shulman GL (2001) A default mode of brain function. Proc Natl Acad Sci U S A 98(2):676–682. doi:10.1073/pnas.98.2.676
17. Zang Y, Jiang T, Lu Y, He Y, Tian L (2004) Regional homogeneity approach to fMRI data analysis. NeuroImage 22(1):394–400. doi:10.1016/j.neuroimage.2003.12.030
18. Zang YF, He Y, Zhu CZ, Cao QJ, Sui MQ, Liang M, Tian LX, Jiang TZ, Wang YF (2007) Altered baseline brain activity in children with ADHD revealed by resting-state functional MRI. Brain Dev 29(2):83–91. doi:10.1016/j.braindev.2006.07.002
19. Tian L, Jiang T, Wang Y, Zang Y, He Y, Liang M, Sui M, Cao Q, Hu S, Peng M, Zhuo Y (2006) Altered resting-state functional connectivity patterns of anterior cingulate cortex in adolescents with attention deficit hyperactivity disorder. Neurosci Lett 400(1–2):39–43. doi:10.1016/j.neulet.2006.02.022
20. Liu Y, Wang K, Yu C, He Y, Zhou Y, Liang M, Wang L, Jiang T (2008) Regional homogeneity, functional connectivity and imaging markers of Alzheimer's disease: a review of resting-state fMRI studies. Neuropsychologia 46(6):1648–1656. doi:10.1016/j.neuropsychologia.2008.01.027
21. Cole DM, Smith SM, Beckmann CF (2010) Advances and pitfalls in the analysis and interpretation of resting-state FMRI data. Front Syst Neurosci 4:8. doi:10.3389/fnsys.2010.00008
22. He Y, Zang YF, Jiang TZ, Lu YL, Weng XC (2004) Detection of functional networks in the resting brain. Biomed Imaging Nano Macro IEEE Int Symp 1:980–983. doi:10.1109/ISBI.2004.1398704
23. Margulies DS, Bottger J, Long X, Lv Y, Kelly C, Schafer A, Goldhahn D, Abbushi A, Milham MP, Lohmann G, Villringer A (2010) Resting developments: a review of fMRI post-processing methodologies for spontaneous brain activity. MAGMA 23(5–6):289–307. doi:10.1007/s10334-010-0228-5
24. Liu H, Liu Z, Liang M, Hao Y, Tan L, Kuang F, Yi Y, Xu L, Jiang T (2006) Decreased regional homogeneity in schizophrenia: a resting state functional magnetic resonance imaging study. Neuroreport 17(1):19–22. doi:00001756-200601230-00005
25. Cao Q, Zang Y, Sun L, Sui M, Long X, Zou Q, Wang Y (2006) Abnormal neural activity in children with attention deficit hyperactivity disorder: a resting-state functional magnetic resonance imaging study. Neuroreport 17(10):1033–1036. doi:10.1097/01.wnr.0000224769.92454.5d

26. American Psychiatric Association (2000) Diagnostic and Statistical Manual of Mental Disorders, 4th ed. American Psychiatric Press: Washington, DC
27. Gabriel SB, Schaffner SF, Nguyen H, Moore JM, Roy J, Blumenstiel B, Higgins J, DeFelice M, Lochner A, Faggart M, Liu-Cordero SN, Rotimi C, Adeyemo A, Cooper R, Ward R, Lander ES, Daly MJ, Altshuler D (2002) The structure of haplotype blocks in the human genome. Science 296(5576):2225–2229. doi:10.1126/science.1069424
28. Donohoe G, Morris DW, Robertson IH, McGhee KA, Murphy K, Kenny N, Clarke S, Gill M, Corvin AP (2007) DAOA ARG30LYS and verbal memory function in schizophrenia. Mol Psychiatry 12 (9):795–796. doi:10.1038/sj.mp. 4002026
29. Craddock N, Owen MJ (2005) The beginning of the end for the Kraepelinian dichotomy. Br J Psychiatry 186:364–366. doi:10.1192/bjp. 186.5.364
30. Gomez L, Wigg K, Feng Y, Kiss E, Kapornai K, Tamas Z, Mayer L, Baji I, Daroczi G, Benak I, Kothencne VO, Dombovari E, Kaczvinszk E, Besnyo M, Gadoros J, King N, Szekely J, Kovacs M, Vetro A, Kennedy JL, Barr CL (2009) G72/G30 (DAOA) and juvenile-onset mood disorders. Am J Med Genet B Neuropsychiatr Genet 150B(7):1007–1012. doi:10.1002/ajmg.b.30904
31. Gawlik M, Wehner I, Mende M, Jung S, Pfuhlmann B, Knapp M, Stober G (2010) The DAOA/G30 locus and affective disorders: haplotype based association study in a polydiagnostic approach. BMC Psychiatry 10:59. doi:10.1186/1471-244X-10-59
32. Grigoroiu-Serbanescu M, Herms S, Diaconu CC, Jamra RA, Meier S, Bleotu C, Neagu AI, Prelipceanu D, Sima D, Gherghel M, Mihailescu R, Rietschel M, Nothen MM, Cichon S, Muhleisen TW (2010) Possible association of different G72/G30 SNPs with mood episodes and persecutory delusions in bipolar I Romanian patients. Prog Neuropsychopharmacol Biol Psychiatry 34(4):657–663. doi:10.1016/j.pnpbp. 2010.03.008
33. Nicodemus KK, Kolachana BS, Vakkalanka R, Straub RE, Giegling I, Egan MF, Rujescu D, Weinberger DR (2007) Evidence for statistical epistasis between catechol-*O*-methyltransferase (COMT) and polymorphisms in RGS4, G72 (DAOA), GRM3, and DISC1: influence on risk of schizophrenia. Hum Genet 120(6):889–906. doi:10.1007/s00439-006-0257-3
34. Shin HD, Park BL, Kim EM, Lee SO, Cheong HS, Lee CH, Kim SG, Sohn JW, Park CS, Kim JW, Kim BH, Kim IY, Choi IG, Woo SI (2007) Association analysis of G72/G30 polymorphisms with schizophrenia in the Korean population. Schizophr Res 96(1–3):119–124. doi:10.1016/j.schres.2007.05.004
35. Schultz CC, Nenadic I, Koch K, Wagner G, Roebel M, Schachtzabel C, Muhleisen TW, Nothen MM, Cichon S, Deufel T, Kiehntopf M, Rietschel M, Reichenbach JR, Sauer H, Schlosser RG (2011) Reduced cortical thickness is associated with the glutamatergic regulatory gene risk variant DAOA Arg30Lys in schizophrenia. Neuropsychopharmacology 36(8):1747–1753. doi:10.1038/npp. 2011.56
36. Soronen P, Silander K, Antila M, Palo OM, Tuulio-Henriksson A, Kieseppa T, Ellonen P, Wedenoja J, Turunen JA, Pietilainen OP, Hennah W, Lonnqvist J, Peltonen L, Partonen T, Paunio T (2008) Association of a nonsynonymous variant of DAOA with visuospatial ability in a bipolar family sample. Biol Psychiatry 64(5):438–442. doi:10.1016/j.biopsych.2008.03.028
37. Shulman RG, Hyder F, Rothman DL (2001) Cerebral energetics and the glycogen shunt: neurochemical basis of functional imaging. Proc Natl Acad Sci U S A 98(11):6417–6422. doi:10.1073/pnas.101129298
38. Liao W, Chen H, Feng Y, Mantini D, Gentili C, Pan Z, Ding J, Duan X, Qiu C, Lui S, Gong Q, Zhang W (2010) Selective aberrant functional connectivity of resting state networks in social anxiety disorder. NeuroImage 52(4):1549–1558. doi:10.1016/j.neuroimage.2010.05.010
39. Greicius MD, Kiviniemi V, Tervonen O, Vainionpaa V, Alahuhta S, Reiss AL, Menon V (2008) Persistent default-mode network connectivity during light sedation. Hum Brain Mapp 29(7):839–847. doi:10.1002/hbm.20537
40. Lorenzi M, Beltramello A, Mercuri NB, Canu E, Zoccatelli G, Pizzini FB, Alessandrini F, Cotelli M, Rosini S, Costardi D, Caltagirone C, Frisoni GB (2011) Effect of memantine on resting state default mode network activity in Alzheimer's disease. Drugs Aging 28(3):205–217. doi:10.2165/11586440-000000000-00000
41. Lyoo IK, Yoon SJ, Musen G, Simonson DC, Weinger K, Bolo N, Ryan CM, Kim JE, Renshaw PF, Jacobson AM (2009) Altered prefrontal glutamate–glutamine–gamma-aminobutyric acid levels and relation to low cognitive performance and depressive symptoms in type 1 diabetes mellitus. Arch Gen Psychiatry 66(8):878–887. doi:10.1001/archgenpsychiatry.2009.86
42. Bechtholt-Gompf AJ, Walther HV, Adams MA, Carlezon WA Jr, Ongur D, Cohen BM (2010) Blockade of astrocytic glutamate uptake in rats induces signs of anhedonia and impaired spatial memory. Neuropsychopharmacology 35(10):2049–2059. doi:10.1038/npp. 2010.74
43. Otte DM, Sommersberg B, Kudin A, Guerrero C, Albayram O, Filiou MD, Frisch P, Yilmaz O, Drews E, Turck CW, Bilkei-Gorzo A, Kunz WS, Beck H, Zimmer A (2011) *N*-acetyl cysteine treatment rescues cognitive deficits induced by mitochondrial dysfunction in G72/G30 transgenic mice. Neuropsychopharmacology 36 (11):2233–2243. doi:10.1038/npp. 2011.109
44. Nandhu MS, Paul J, Kuruvila KP, Abraham PM, Antony S, Paulose CS (2011) Glutamate and NMDA receptors activation leads to cerebellar dysfunction and impaired motor coordination in unilateral 6-hydroxydopamine lesioned Parkinson's rat: functional recovery with bone marrow cells, serotonin and GABA. Mol Cell Biochem 353(1–2):47–57. doi:10.1007/s11010-011-0773-x
45. Rapoport M, van Reekum R, Mayberg H (2000) The role of the cerebellum in cognition and behavior: a selective review. J Neuropsychiatry Clin Neurosci 12(2):193–198
46. Liu Z, Xu C, Xu Y, Wang Y, Zhao B, Lv Y, Cao X, Zhang K, Du C (2010) Decreased regional homogeneity in insula and cerebellum: a resting-state fMRI study in patients with major depression and subjects at high risk for major depression. Psychiatry Res 182 (3):211–215. doi:10.1016/j.pscychresns.2010.03.004
47. Otte DM, Bilkei-Gorzo A, Filiou MD, Turck CW, Yilmaz O, Holst MI, Schilling K, Abou-Jamra R, Schumacher J, Benzel I, Kunz WS, Beck H, Zimmer A (2009) Behavioral changes in G72/G30 transgenic mice. Eur Neuropsychopharmacol 19(5):339–348. doi:10.1016/j.euroneuro.2008.12.009
48. Langenecker SA, Kennedy SE, Guidotti LM, Briceno EM, Own LS, Hooven T, Young EA, Akil H, Noll DC, Zubieta JK (2007) Frontal and limbic activation during inhibitory control predicts treatment response in major depressive disorder. Biol Psychiatry 62(11):1272–1280. doi:10.1016/j.biopsych.2007.02.019
49. Siok WT, Perfetti CA, Jin Z, Tan LH (2004) Biological abnormality of impaired reading is constrained by culture. Nature 431 (7004):71–76. doi:10.1038/nature02865
50. Krug A, Markov V, Krach S, Jansen A, Zerres K, Eggermann T, Stocker T, Shah NJ, Nothen MM, Georgi A, Strohmaier J, Rietschel M, Kircher T (2011) Genetic variation in G72 correlates with brain activation in the right middle temporal gyrus in a verbal fluency task in healthy individuals. Hum Brain Mapp 32(1):118–126. doi:10.1002/hbm.21005
51. Li D, Huang X, Wu Q, Zou K, Sun X, Gong Q (2010) Brain functions in major depressive disorder: a resting-state functional magnetic resonance imaging study. Sheng Wu Yi Xue Gong Cheng Xue Za Zhi 27(1):16–19
52. De Kloet ER, Reul JM (1987) Feedback action and tonic influence of corticosteroids on brain function: a concept arising from the

heterogeneity of brain receptor systems. Psychoneuroendocrinology 12(2):83–105

53. Aston C, Jiang L, Sokolov BP (2005) Transcriptional profiling reveals evidence for signaling and oligodendroglial abnormalities in the temporal cortex from patients with major depressive disorder. Mol Psychiatry 10(3):309–322. doi:10.1038/sj.mp. 4001565
54. Hasler G, van der Veen JW, Tumonis T, Meyers N, Shen J, Drevets WC (2007) Reduced prefrontal glutamate/glutamine and gamma-aminobutyric acid levels in major depression determined using proton magnetic resonance spectroscopy. Arch Gen Psychiatry 64(2):193–200. doi:10.1001/archpsyc.64.2.193
55. Walter M, Henning A, Grimm S, Schulte RF, Beck J, Dydak U, Schnepf B, Boeker H, Boesiger P, Northoff G (2009) The relationship between aberrant neuronal activation in the pregenual anterior cingulate, altered glutamatergic metabolism, and anhedonia in major depression. Arch Gen Psychiatry 66 (5):478–486. doi:10.1001/archgenpsychiatry.2009.39
56. Kiss JP, Szasz BK, Fodor L, Mike A, Lenkey N, Kurko D, Nagy J, Vizi ES (2012) GluN2B-containing NMDA receptors as possible targets for the neuroprotective and antidepressant effects of fluoxetine. Neurochem Int 60(2):170–176. doi:10.1016/j.neuint.2011.12.005
57. Barbon A, Caracciolo L, Orlandi C, Musazzi L, Mallei A, La Via L, Bonini D, Mora C, Tardito D, Gennarelli M, Racagni G, Popoli M, Barlati S (2011) Chronic antidepressant treatments induce a time-dependent up-regulation of AMPA receptor subunit protein levels. Neurochem Int 59(6):896–905. doi:10.1016/j.neuint.2011.07.013
58. Northoff G, Walter M, Schulte RF, Beck J, Dydak U, Henning A, Boeker H, Grimm S, Boesiger P (2007) GABA concentrations in the human anterior cingulate cortex predict negative BOLD responses in fMRI. Nat Neurosci 10 (12):1515–1517. doi:10.1038/nn2001